Aerospace Science and Technology 73 (2018) 332–342

Contents lists available at ScienceDirect

Aerospace Science and Technology

www.elsevier.com/locate/aescte

Numerical investigation of the axial impulse load during the startup in the shock tunnel

Baoqing Meng [a,b], Guilai Han [a,b,*], Changtong Luo [a,b], Zonglin Jiang [a,b]

[a] *State Key Laboratory of High-temperature Gas Dynamics, Institute of Mechanics, Chinese Academy of Sciences, 100190 Beijing, China*
[b] *University of Chinese Academy of Sciences, 100049 Beijing, China*

ARTICLE INFO

Article history:
Received 15 May 2017
Received in revised form 1 December 2017
Accepted 7 December 2017
Available online 13 December 2017

Keywords:
Hypersonic
Shock tunnel
Start-up process
Impulse force
Vibration

ABSTRACT

A shock tunnel is a representative type of ground-based equipment in the hypersonic field, which has the advantage of free stream of excellent quality. Accurate measurements of aerodynamic forces in the shock tunnel are great challenges. The impulse loads during the start-up process induce the vibration of the model and its support. Aerodynamic signals are disturbed by vibrational signals. The identification of the starting time of the steady periodic vibration and excited natural frequencies of the whole structure would contribute to improve the accuracy of measurement. These two factors are closely related to the properties of the impulse forces. However, there is currently no published research on the impulse forces. In this paper, the type of impulse forces (drag history) acting on the sharp cone during the start-up process was investigated by numerical simulation. The distribution of the static pressure of the typical wave structures was found to have a significant influence on the types of the drag history. A formula, based on the physical analysis of start-up process, was put forward to estimate the starting time of the steady stage. Additionally, the subsequent analysis and design optimization such as vibration of structure and disturbing frequencies needed an analytical and simple formation of drag history. Thus, the drag history was approximated by numbers of sine functions. Different phases exhibited notable difference in composition. Also, a metric denoted as the energy coefficient was derived to identify the critical frequencies and simplify the analytical expression of the impulse force.

1. Introduction

A shock tunnel is a representative type of ground-based equipment in the hypersonic field, which has the advantages of high total pressure, high total temperature and low cost. As a typical piece of impulse equipment, the operational time of a shock tunnel is extremely short, with a test time that is usually in the range of 2–30 ms [1,2]. Such a short running time constitutes a great challenge regarding the accurate measurement of the aerodynamic force. For a conventional tunnel, the running time is generally several minutes, i.e., a much longer time than the vibration period of the force measurement structure, which includes a sting support, measurement components and the aircraft model. The effects of damping are obvious, and the whole structure can reach a force equilibrium condition. The measurement is quasi-static, and the high accuracy of the measurement can be ensured, but, there are essential differences for the force measurements in the shock tunnel. Nevertheless, the effects of vibration damping can be neglected because the order of magnitude of the test time is the same as that of the period of the force measurement structure. Therefore, the measurement of the balance of aerodynamic forces is a dynamic process. In addition, only several periods of signals can be obtained from the outputs of the balance. Also, due to the essentially different mechanical state of the force measurement systems during testing, the difficulty and accuracy of the force measurement in the shock tunnel are evidently different from those in a conventional tunnel.

The vibration of the force measurement structure in the shock tunnel is initiated by the impulse aerodynamic force during the nozzle start-up process, and the whole structure reaches a steady periodic vibration around the equilibrium position during the test period. The signals sensed by the balance are a combination of the aerodynamic force signals and vibrational signals. The removal of the vibrational signals is essential for force signal processing in the shock tunnel. Several methods have been developed for the peeling of the signals, including one technique that is commonly used, namely the acceleration compensation force balance technique [3–7]. The accelerometers are mounted near the measurement component and the acceleration signals are measured

* Corresponding author at: State Key Laboratory of High-temperature Gas Dynamics, Institute of Mechanics, Chinese Academy of Sciences, 100190 Beijing, China.
E-mail address: hanguilai@imech.ac.cn (G. Han).

https://doi.org/10.1016/j.ast.2017.12.013
1270-9638/

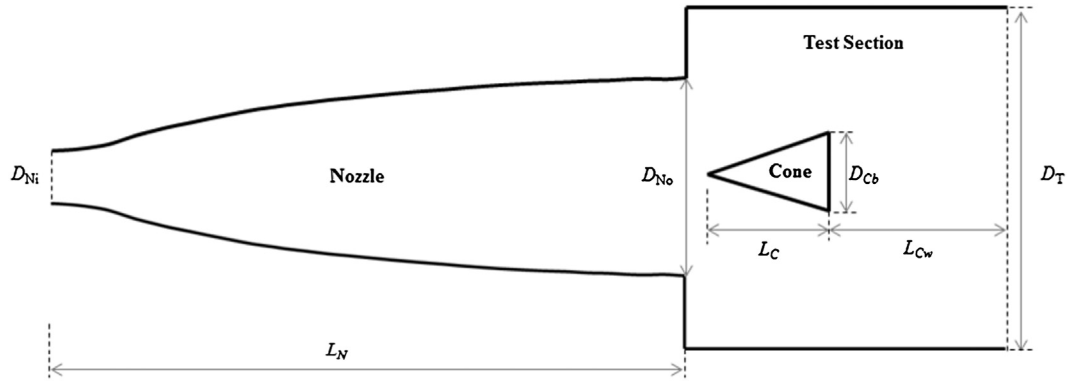

Fig. 1. Schematic drawing of the computational domain.

along with the force signals. The plat force signals are obtained by adding the processed acceleration signals to the force signals. The acceleration signals supplied by accelerators can only display the frequencies of free vibration properties at a certain position with very limited information on the vibration. Another method involves using the average to counteract the fluctuation of the selected signals. For both of these methods, the detailed understanding of the starting time of the steady periodic duration and disturbing frequencies are very important to ensure the accuracy of the force measurements. The start-up stage and the following steady vibration comprise the whole process of the tunnel test. The starting time point is just the end of the start-up stage. Accordingly, the time of duration of the impulse force should be identified. Also, the vibrational theory indicates that the initial condition of the steady vibration depends on the start-up stage. Thus, the form and frequency composition of the impulse force need to be investigated. However, no research on the characteristics of the impulse forces during start-up of shock tunnel has been reported to date.

Meanwhile, the wave structures of the nozzle start-up process have been investigated in numerous studies involving a shock tunnel [8–14]. Typical wave structures consisting of primary shock (PS), secondary shock (SS) and contact discontinuity (CD) have been observed during the start-up process of the nozzle of the shock tunnel. The typical wave structures indicate that the pressure distribution around the center zone of the nozzle has a certain commonality for different nozzles in a shock tunnel. Thus, common characteristics exist for the impulse drag-time curve acting on an aircraft model.

This paper described the study of the various characteristics of an axial impulse force history acting on a sharp cone during the start-up process of the JF12 shock tunnel. The JF12 hypersonic shock tunnel was successfully developed by Jiang et al. [15] at the Institute of Mechanics Chinese Academy of Sciences (CAS). The wave structures and mechanisms of the impulse force were also investigated. A formula based on the physical analysis of the start-up process, was put forward to estimate the starting time of the steady stage. Furthermore, the subsequent analysis and design optimization such as vibration of structure and disturbing frequencies needed an analytical and simple formation of drag history. Additionally, analytical modeling with numbers of sine functions for the impulse force was conducted, this approach made the theoretical study of the subsequent analysis of the vibrational properties possible. Further studies aimed at simplifying the analytical form of impulse force were also conducted. The simplification should be based on a metric to identify the critical frequencies. A metric denoted as the energy coefficient was derived based on the vibrational theory. The number of the sine functions was replaced by only three significant sine functions and an acceptable substitution effect was obtained.

Table 1
Dimension of the computational domain.

Definition	Dimension (mm)
D_{Ni}	310.0
D_{No}	2457.8
L_N	14250.0
D_{Cb}	529.0
L_C	1500.0
D_T	3500.0

2. Numerical method

2.1. Computational domain and grid generation

The computational domain contains a nozzle of 14.2 m in length and 2.5 m in diameter, a test section and a sharp cone with a semi angle of 10°, as shown in Fig. 1. **The calibrated results of the flow showed that the deviation of the Mach number around the effective region of the nozzle outlet was less than 2%.** The flow was simplified to be axisymmetric and the computational domain was simplified to a two-dimensional region. Only the properties of the axis forces were of interest in the current study and the effects of the flow asymmetry were beyond the scope of this research. The detailed dimensions of each section are listed in Table 1. L_N, L_C and L_{cw} denote the length of the nozzle, sharp-cone, and wake region, respectively; D_{Ni}, D_{No}, D_{Cb} and D_T represent the diameters of the nozzle throat, nozzle outlet, cone base and test section, respectively.

The whole domain was divided into six blocks for grid generation and computational purposes, as shown in Fig. 2. Because the finite difference method and structural meshes were used, mesh orthogonality was important to achieve an accurate calculation. An orthogonal mesh approach proposed by Volkan Akcelik [16] was used for grid generation; this method ensured the mesh orthogonality in the inner flow field. In addition, the mesh orthogonality near the wall was also ensured by creating vertical lines to the boundary lines passing through the inner gird points. A total of five separate grids were used for grid independence verification. Each grid described in Table 2 was obtained from the previous grid by doubling the number of grids in the i and j directions.

2.2. Governing equation and algorithm

The two-dimensional axisymmetric and compressible Navier–Stokes equations with transformation to the computational space [17] presented in eq. (1) were used for the calculation. The convective term was solved using the NND scheme [18], and the viscous term was discretized using the second-order central difference method. The first-order Runge–Kutta method was applied